

OPTIMAL DESIGN OF PNEUMATIC BALANCING MECHANISM FOR POWER ASSISTED MANIPULATOR

Xinglei ZHANG^{1, 3*}, Binghui FAN^{2*}, Chuanjiang WANG²

The supporting force of pneumatic balancing mechanism of power assisted manipulator is constant or the installation parameters are random. These two situations will lead to the decline of assist effect when assist manipulator operates different gravity loads. Therefore, an optimized design scheme for pneumatic balancing mechanism of assist manipulator is proposed. First, in the rated load state, the absolute value of the difference between the balance torque and the gravitational moment of load is established as the objective function. The constraint function is created according to the working performance of pneumatic balance mechanism and the requirement that the manipulator motion process cannot interfere. The optimal installation parameters of pneumatic balancing mechanism are obtained by the constrained nonlinear optimization algorithm in MATLAB. Then, according to the different gravity loads, the supporting forces by pneumatic balancing mechanism are optimized, and the distribution of driving torque of the motor with during the working process of the assisted manipulator are obtained. The optimization results show that power assisted manipulator only needs to provide a small driving torque to complete the transportation of large load, and improve the power assisted effect of the manipulator.

Keywords: power assisted manipulator, gravitational torque balance, pneumatic balance mechanism, optimization method.

1. Introduction

Although more and more robotic equipment has kept workers away from labor-intensive working environments, robots cannot completely replace humans in some complex environments. A device that can minimize the amount of labor and give full play to people's subjective initiative is necessary. Power assisted manipulator which can give full play to the respective advantages of human and machine each other can fill this gap [1]. Power assisted manipulator often makes pitching motions under no load or different loads. There must be a problem of

¹College of Mechanical and Electronic Engineering, Shandong University of Science and Technology, Qingdao, 266590, China.

²College of Electrical and Automation Engineering, Shandong University of Science and Technology, Qingdao, 266590, China.

³College of Mechanical and Electronic Engineering, Zaozhuang University, Zaozhuang, 277160, China.

*Email: zhangxingfulove@163.com, fbxzxl@126.com

overcoming the gravity moment of the manipulator and the load. When power assisted manipulator faces a load with low gravity, it can be powered by the motor to complete the work. However, when facing a load with heavy gravity, a large motor is needed to provide power, which increases the cost of equipment.

Common gravity compensation methods for manipulators include counterweights, springs, pneumatic or hydraulic cylinders, and electromagnetic devices [2]. In [3], the unbalance of the gravitational moment generated during the operation of the eccentric is overcome by the counterweight method. Singh et al [4] designed suitable springs to provide resistance to torque. In [5], an auxiliary balance system composed of the pantograph linkage mechanism were utilized for the balance of the manipulator, which reduced the load of the robot actuator. Lee et al [6] used a constant force spring and balance mechanism for gravity compensation on the positioning link. Morita et al. [7] proposed a multi-DOF counterbalance mechanism using a pseudo parallelogram mechanism based on a belt and pulley. In [8], spring-based gravity compensation was applied to the pitch joints of a 4-DOF flexible surgical instrument to reduce wrist fatigue. Koser [9] designed a cam-type counterbalance mechanism for industrial manipulators. Kim [10] presented a novel counterbalance mechanism composed of springs and double parallelogram mechanisms.

However, the supporting force of the pneumatic balancing device commonly used in the past is constant or the installation parameters of the balancing mechanism are random. When the load gravity of the manipulator changes, the requirement of gravity moment balance cannot be well achieved. In this way, the driving device needs to provide a larger output torque to meet the work requirements of the manipulator. How to make the balance device provide a more precise balance torque to reduce the output torque of the driving device and expand the load range of the manipulator is a problem that needs to be solved. Therefore, the balance device is optimized to obtain the installation parameters and supporting force to achieve the purpose of power assisted manipulator to effectively balance the gravitational moment of the manipulator and load.

2. Balancing principle

Power assisted manipulator is used to grasp and carry objects, mainly including a manipulator base, a big arm, a balancing mechanism, a forearm, and a gripper [11]. The big arm is installed on the manipulator base, and the pneumatic balancing mechanism is installed on the big arm and base. The forearm is hinged with the big arm and the gripper is mounted on the forearm. Through the rotation of the big arm and the forearm and combined with the horizontal rotation of the manipulator base, the gripper can realize the movement in Cartesian space.

The balance device of power assisted manipulator studied in this paper selects a pneumatic balance mechanism, which is hinged on the big arm and

manipulator base. When the big arm is pitching, the pneumatic balance mechanism will expand and contract to produce a pulling force. At this time, the torque generated by the pulling force can balance the gravitational moment of the manipulator and load to a large extent. Therefore, the driving torque of the motor required is greatly reduced. The structure diagram of power assisted manipulator is shown in Fig. 1.

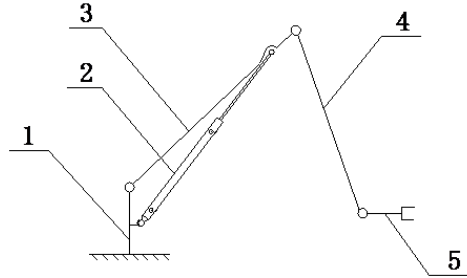


Fig. 1. The structure diagram of power assisted manipulator. 1. manipulator base, 2. pneumatic balance mechanism, 3. big arm, 4. forearm, 5. gripper

3. Establishing optimization design model

Due to the limited pressure value of the pneumatic balance mechanism, the driving force of the cylinder should not be too large. In the case of meeting the working requirements of the assisted manipulator, in order to make the motor driving force as small as possible, a strategy to obtain the optimal installation parameters of the pneumatic balancing mechanism is proposed.

The force mathematical model of power assisted manipulator is shown in Fig. 2. To complete the effective use of pneumatic balancing mechanism, four parameters X_1 , X_2 , X_3 , X_4 need to be obtained. Among them, $X_1 = LM$, $X_2 = OL$, $X_3 = ON$, X_4 is the supporting force of pneumatic balancing mechanism; The value range of the angle α with the horizontal plane during the pitching movement of the big arm is $[30^\circ, 90^\circ]$, and the value range of the angle β with the horizontal plane during the pitching movement of the forearm is $[-30^\circ, 30^\circ]$.

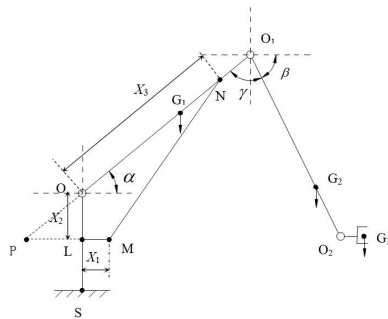


Fig. 2. The force mathematical model diagram of power assisted manipulator

In this paper, the length of the big arm, $OO_1=1.2\text{m}$; the length from the big arm pitch joint O to the big arm center of gravity G_1 , $OG_1=0.6\text{m}$; the manipulator forearm length, $O_1G_3=1.2\text{m}$; the length from the forearm pitch joint O_1 to the forearm center of gravity G_2 , $O_1G_2=0.7\text{m}$; the length from the manipulator joint O_2 to the gripper and the load center of gravity G_3 , $O_2G_3=0.25\text{m}$; the big arm mass, $m_1 = 30\text{kg}$; forearm mass, $m_2 = 30\text{kg}$; gripper mass, $m_3 = 10\text{kg}$; rated load mass, $m_4^* = 200\text{kg}$.

Under the condition of rated load, the absolute value of the difference between the balance moment generated by the pneumatic balance mechanism and the total weight moment of the arm and load is established as the objective function. According to the structure of the manipulator, the working performance of the pneumatic balancing mechanism, and the requirement that no interference occurs during the motion of the assisted manipulator, the constraint function are as follows:

$$0.01 \leq X_1 \leq 0.4 \text{ (m)} \quad (1)$$

$$0.01 \leq X_2 \leq 0.3 \text{ (m)} \quad (2)$$

$$0.1 \leq X_3 \leq 0.7 \text{ (m)} \quad (3)$$

$$10 \leq X_4 \leq 36000 \text{ (N)} \quad (4)$$

The mathematical model of the balancing torque of pneumatic balancing mechanism M_p , the pitching gravity moment M_d of the big arm, the pitching gravity moment M_x of the forearm, the gravity moment M_f of the gripper and the load are established as follows.

$$M_d = m_1 \cdot g \cdot L_d \quad (5)$$

$$M_x = m_2 \cdot g \cdot L_x \quad (6)$$

$$M_f = (m_3 + m_4) \cdot g \cdot L_f \quad (7)$$

$$M_p = X_4 \cdot L_p \quad (8)$$

$$L_d = OG_1 \cdot \cos\alpha \quad (9)$$

$$L_x = OO_1 \cdot \cos\alpha + O_1G_2 \cdot \cos\beta \quad (10)$$

$$PM = X_1 + X_2 / \tan\alpha \quad (11)$$

$$PN = X_3 + X_2 / \sin\alpha \quad (12)$$

$$MN = \sqrt{PM^2 + PN^2 - 2 \cdot PM \cdot PN \cdot \cos\alpha} \quad (13)$$

$$\angle ONM = \arcsin\left(\frac{PM \cdot \sin\alpha}{MN}\right) \quad (14)$$

$$L_p = X_3 \cdot \sin \angle OMN \quad (15)$$

$$L_f = OO_1 \cdot \cos \alpha + O_1 G_2 \cdot \cos \beta + O_2 G_3 \quad (16)$$

Where L_d is the force arm of the big arm gravity, L_x is the force arm of the forearm gravity, L_f is the force arm of the gripper and load. L_p is the force arm of the pneumatic balance mechanism, MN is the length of pneumatic balancing mechanism. When the big arm and forearm are pitching, an objective function is established to minimize the maximum absolute value of the difference between the balance torque generated by the pneumatic balancing mechanism and the total weight torque.

$$f(x) = \max(\text{abs}(\Delta M)) \quad (17)$$

$$f_{\min}(x) = \min(f(x)) \quad (18)$$

Where $\Delta M = M_d + M_x + M_f - M_p$, it represents the difference between the balancing torque generated by the pneumatic balancing mechanism and the total weight torque at each angle during the pitching motion of the big arm and the forearm under the condition of rated load.

$f(x)$ intends the maximum absolute value of ΔM at each discrete position of the manipulator.

$f_{\min}(x)$ is the objective function, and the optimization design is to make $f_{\min}(x)$ minimum, *i.e.*, the motor driving torque required by the power assisted manipulator is minimum.

4. Parameter optimization and simulation

The design parameters X_1 , X_2 , X_3 , X_4 are optimized by the constrained nonlinear optimization algorithm [13] in MATLAB optimization design, and the optimization results of each design parameter and objective function are as follows:

$$X_1 = 0.3 \text{m} ; \quad X_2 = 0.27 \text{m} ; \quad X_3 = 0.49 \text{m} ; \quad X_4 = 16900 \text{N} ;$$

$$f_{\min}(x) = 204 \text{Nm}$$

Furthermore, the distribution of the driving torque of the motor with the change of α and β are obtained with and without the pneumatic balancing mechanism as shown Fig.3. Without installing the pneumatic balancing mechanism, the driving torque is up to 5787Nm by the motor during the working process of the power assisted manipulator as shown in Fig. 3 (a). However, with installing the pneumatic balancing mechanism, the value is reduced to 204 Nm, as shown in Fig. 3 (b), and the torque balance rate can reach 96.5%. In the range of motion of the power assisted manipulator, 25 positions are randomly selected, and

their torque balance rates are obtained, as shown in Fig. 4. It is found that torque balance rates are between 93.7% and 99.8%, so the weight torque is effectively balanced.

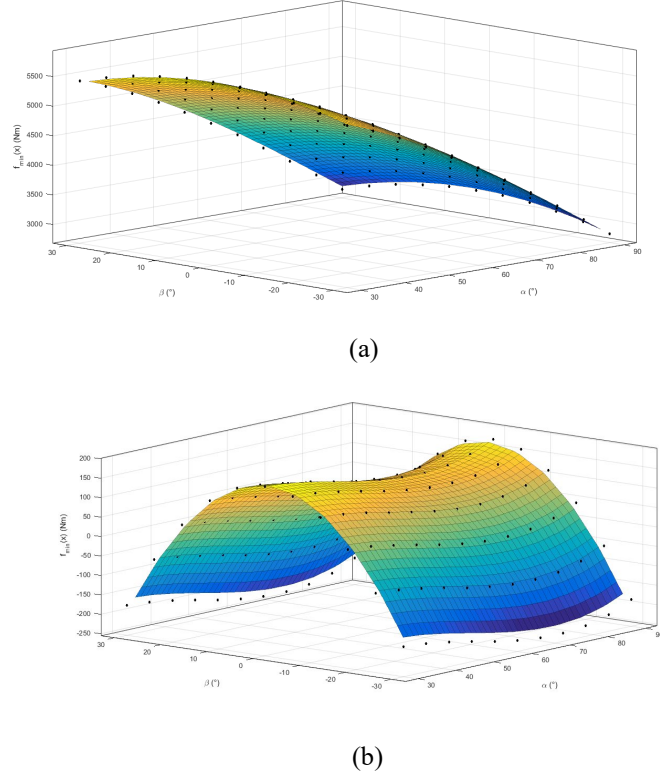


Fig. 3. (a) As $m_4^* = 200\text{kg}$, motor output driving torque without pneumatic balancing mechanism for power assisted manipulator; (b) Motor output driving torque with pneumatic balancing mechanism for power assisted manipulator

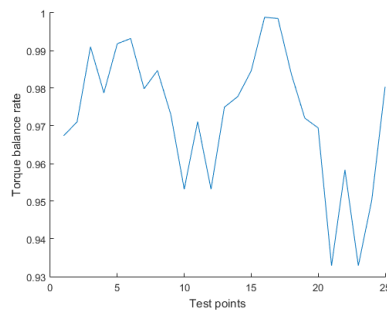


Fig. 4. As $m_4^* = 200\text{kg}$, torque balance rate of test positions

Then, on the basis of X_1 , X_2 , and X_3 , m_4 is take as 0kg, 50kg, 100kg, 150kg, respectively. $f_{\min}(x)$ continues to be as objective function to optimize X_4 .

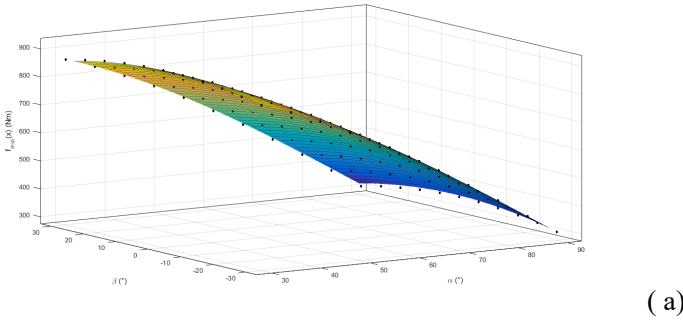
The maximum driving torque (with and without the pneumatic balancing mechanism) and the torque balance rate are also got, as shown in Table 1. The corresponding distribution of the driving torque of the motor with the change of α and β are obtained with and without the pneumatic balancing mechanism as shown Figs. 5, 7, 9, 11.

Table 1

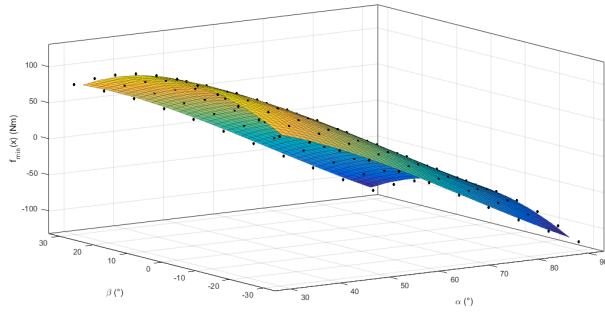
Optimized results

m_4 (kg)	$f_{\min}(x)$ (Nm)	$M_d + M_x + M_f$ (Nm)	Torque balance rate	X_4 (N)	Motor output drive torque
0	120	908	86.8%	2377	Fig. 5
50	136	2128	93.6%	6006	Fig. 7
100	154	3347	95.4%	9629	Fig. 9
150	180	4567	96%	13225	Fig. 11
200	204	5787	96.5%	16900	Fig. 3

From Table 1, it can be seen that the maximum driving torque of the motor needs to be increased from 908Nm to 5787Nm without installing the pneumatic balancing mechanism. However, the maximum driving torque of the motor only needs to be increased from 120Nm to 204Nm with installing the pneumatic balance mechanism. At this time, X_4 needs to be increased from 2377N to 16900N to achieve this effect.



(a)



(b)

Fig. 5. (a) As $m_4 = 0$ kg , motor output driving torque with the pneumatic balancing mechanism for power assisted manipulator; (b) Motor output driving torque without the pneumatic balancing mechanism for power assisted manipulator

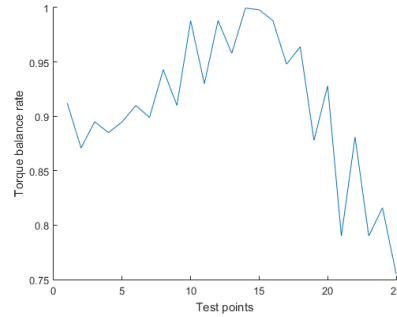


Fig. 6. As $m_4 = 0\text{kg}$, torque balance rate of test points

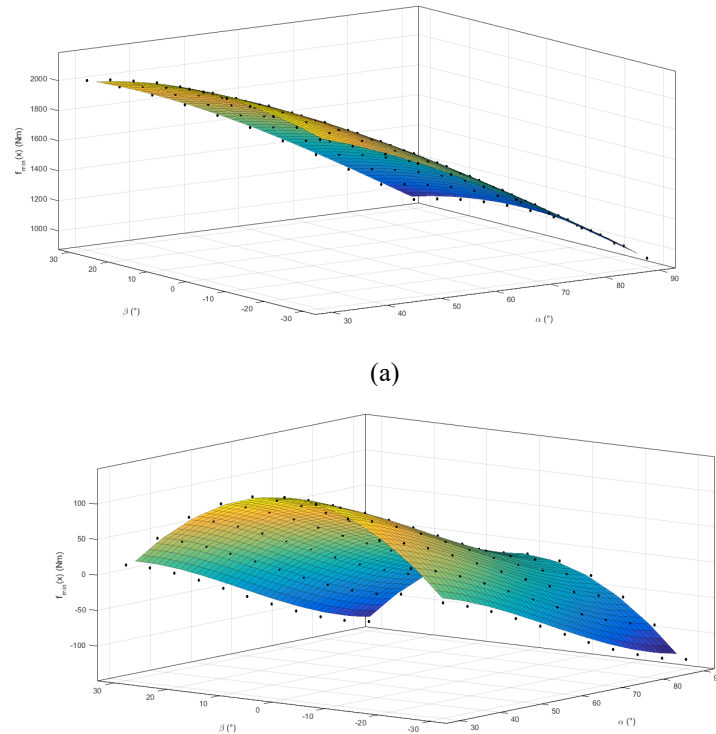
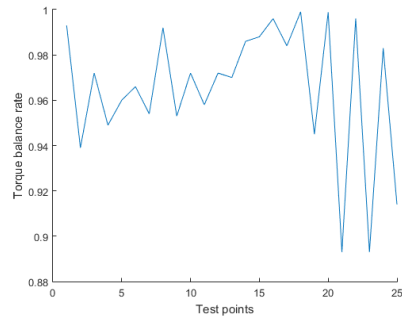
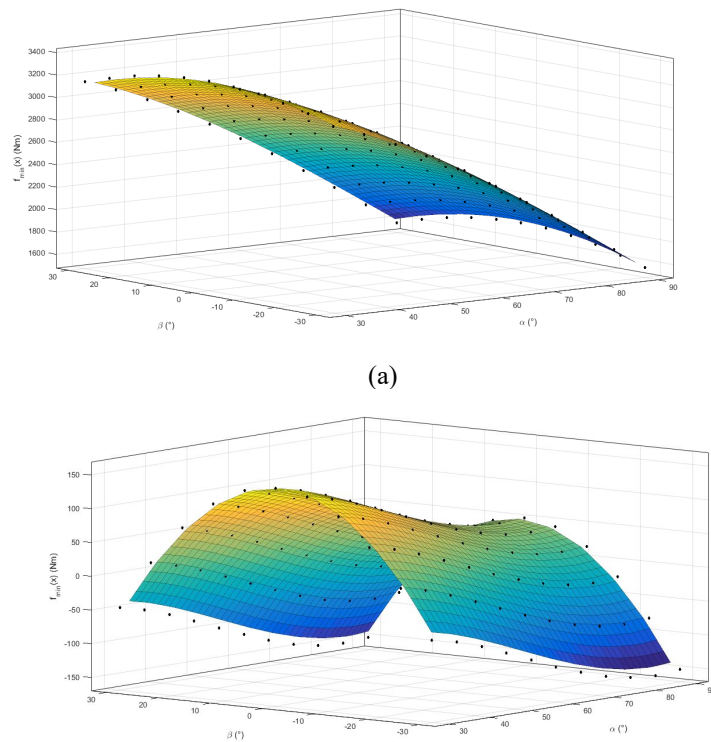


Fig. 7. (a) As $m_4 = 50\text{kg}$, motor output driving torque without the pneumatic balancing mechanism for power assisted manipulator; (b) Motor output driving torque with the pneumatic balancing mechanism for power assisted manipulator

Fig. 8. As $m_4 = 50\text{kg}$, torque balance rate of test pointFig. 9. (a) As $m_4 = 100\text{kg}$, motor output driving torque with the pneumatic balancing mechanism for power assisted manipulator; (b) Motor output driving torque without the pneumatic balancing mechanism for power assisted manipulator

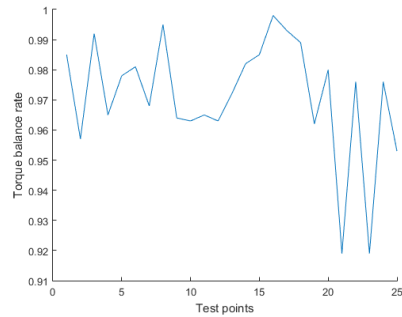


Fig. 10. As $m_4 = 100\text{kg}$, torque balance rate of test point

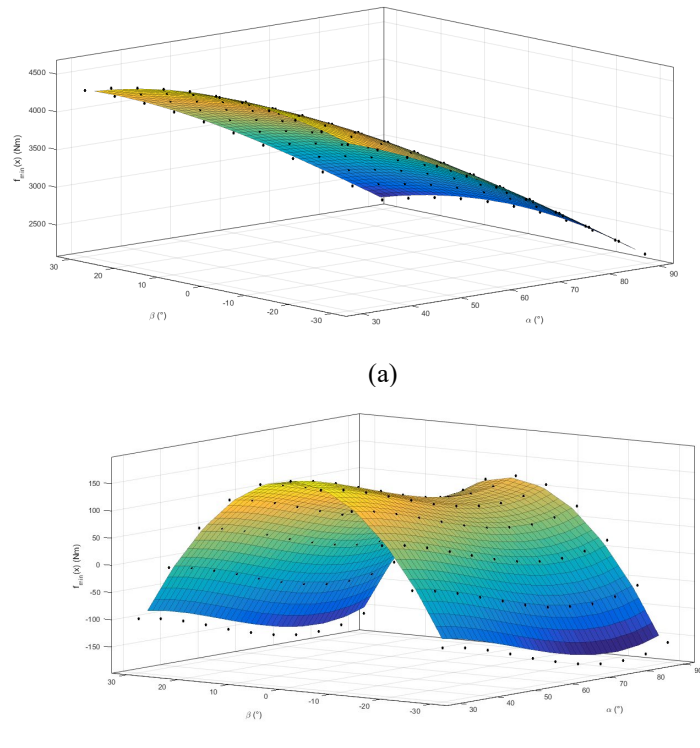


Fig. 11. (a) As $m_4 = 150\text{kg}$, motor output driving torque with the pneumatic balancing mechanism for power assisted manipulator; (b) Motor output driving torque without the pneumatic balancing mechanism for power assisted manipulator

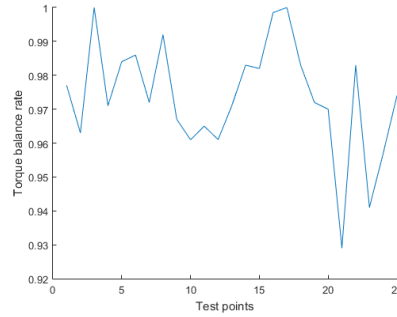


Fig. 12. As $m_4 = 150\text{kg}$, torque balance rate of test points

From Figs. 4, 6, 8, and 12, it is found that the balance rate varies between 75.4% and 99.8% under no load, and the balance rate varies between 89.3% and 100% under load. *i.e.*, the balance effect with load is better than that without load. Figs. 3, 5, 7, 9, 11 show that the motor drive torque varies between 304Nm and 5787 without the pneumatic balance mechanism. However, the motor drive torque only varies between -235Nm and 204 with the pneumatic balance mechanism. The reason for the continuous change of the driving torque is that the direction of the supporting force and the force arm are constantly changing during operation of the assistant manipulator.

5. Conclusions and future work

In view of the poor efficiency of the traditional power assisted manipulators, an optimization scheme for the pneumatic balancing mechanism of power assisted manipulators is proposed. First, a pneumatic balancing mechanism of the assist manipulator is optimized to obtain the best installation parameters under the rated load. On this basis, according to the different load, the supporting force of the pneumatic balancing mechanism is optimized. Finally, the distribution of the driving torque of the motor with the change of α and β is obtained through MATLAB simulation, and torque balance rate of test points are obtained. The simulations show that the motor driving torque varies from -235Nm to 204Nm with pneumatic balancing mechanism. It is much smaller than the range of 908Nm to 5787Nm without pneumatic balancing mechanism. The torque balance rate of test points varies between 75.4% and 100%, and the balance effect with load is better than that without load. The driving torque of motor is greatly reduced, and the power effect of power assisted manipulator is significantly improved.

Simulations show that the range of motor driving torque is a little large. Therefore, in the future, we will try to introduce a closed-loop feedback control algorithm to accurately adjust X_4 to further reduce the motor drive torque and make it change within a small range.

Acknowledgments

This work was supported by the Major Science and Technology Innovation Projects in Shandong Province, China (2017CXGC0919), the National Natural Science Foundation of China Youth Fund (61803235) and the Natural Science Foundation of Shandong Province (under Project No. ZR2020ME252).

R E F E R E N C E S

- [1]. *H. Y. Kuai*, Design and Research of Mechanical Structure for the Automatic Blanking Machine, Taiyuan: North University of China, 2017.
- [2]. *V. Arakelian, S. Briot*. Balancing of linkages and robot manipulators: advanced methods with illustrative examples. Springer International Publishing, 2015.
- [3]. *X. Li, H. Chen, Z. Ye, H. Guo, T. Zou*. “Dynamic balance optimization of the cutting head for flexible materials based on solidworks”, U. P. B., Scientific Bulletin, Series D: Mechanical Engineering, **vol. 81**, no. 3, 2019, pp.3-14.
- [4]. *A. Singh, A. Singla, S. Soni*. “Gravity balancing of a seven- DOFs hybrid manipulator”, In: 2nd International and 17th National Conference on Machines and Mechanisms, Kanpur, Dec. 2015, pp. 5-14.
- [5]. *V. Arakelian, S. Briot*. “Balancing of Manipulators by Using the Copying Properties of Pantograph Mechanisms”, In: Balancing of Linkages and Robot Manipulators. Mechanisms and Machine Science, **vol 27**, Jan. 2015, pp.147-188.
- [6]. *H. Lee, B. Cheon, D. Kim, D. Lee, D. Jeong, M. Hwang, D. Kang, H. Baek, D. S. Kwon*. “Endo-Trainer-A low-cost training system for da Vinci robotic surgery”, International Journal of Computer Assisted Radiology and Surgery, **vol 12**, no. 1, 2017, pp. S244-S245.
- [7]. *T. Morita, F. Kuribara, Y. Shiozawa, S. Sugano*. “A novel mechanism design for gravity compensation in three-dimensional space”, Advanced Intelligent Mechatronics, Proceedings. IEEE/ASME International Conference on, **vol 1**, Aug. 2003, pp. 163-168.
- [8]. *J. Ahn, J. Kim, H. Kim, D. S. Kwon*. “Design of 4-DOFs master device and preliminary test for flexible endoscopic robot surgery”, International Journal of Computer Assisted Radiology and Surgery, **vol 14**, 2019, pp. S146-S147.
- [9]. *K. Koser*. “A cam mechanism for gravity-balancing”, Mechanics Research Communications, **vol 36**, no. 4, June. 2009, pp. 523-530.
- [10]. *H. S. Kim, J. B. Song*. “Multi-DOF Counterbalance Mechanism for a Service Robot Arm”, IEEE/ASME Transactions on Mechatronics, **vol 19**, no. 6, Dec. 2014, pp.1756-1763.
- [11]. *S. D. Sun*. Technical basis of industrial robot, Northwestern Polytechnical University Press, Xi'an, 2007.
- [12]. *C. F. Ma*. Optimization method and its MATLAB program design, Science Press, Beijing, 2010.